Received: 8 September 2022 | Accepted: 6 January 2023

DOI: 10.1097/HEP.0000000000000314

ORIGINAL ARTICLE

OPEN

Hepatic mitochondrial NAD+ transporter SLC25A47 activates AMPKα mediating lipid metabolism and tumorigenesis

Lili Cheng[1,2] | R.N.V. Krishna Deepak[3] | Guoqiang Wang[1] | Ziyi Meng[1] | Lei Tao[1] | Mengqing Xie[1] | Wenna Chi[1] | Yuming Zhang[1] | Mingming Yang[1] | Yilie Liao[4] | Ruiqun Chen[1] | Yu Liang[1] | Junyu Zhang[1] | Yuedong Huang[1] | Weihua Wang[1] | Zhiying Guo[5] | Yunfang Wang[5] | Jiandie D. Lin[6] | Hao Fan[3] | Ligong Chen[1,2,7]

[1]School of Pharmaceutical Sciences, Key Laboratory of Bioorganic Phosphorus Chemistry and Chemical Biology (Ministry of Education), Tsinghua University, Beijing China

[2]Advanced Innovation Center for Human Brain Protection, Beijing Tiantan Hospital, Capital Medical University, Beijing, China

[3]Bioinformatics Institute (BII), Agency for Science, Technology and Research (A*STAR), Singapore

[4]School of Life Sciences, Tsinghua University, Beijing, China

[5]Hepatopancreatobiliary Center, Beijing Tsinghua Changgung Hospital, School of Clinical Medicine, Tsinghua University, Beijing, China

[6]Life Sciences Institute, University of Michigan, Ann Arbor, Michigan, USA

[7]Collaborative Innovation Center for Biotherapy, State Key Laboratory of Biotherapy and Cancer Center, West China Hospital, West China Medical School, Sichuan University, Chengdu, China

Correspondence
Ligong Chen, School of Pharmaceutical Sciences, Tsinghua University, Beijing 100084, China.
E-mail: ligongchen@tsinghua.edu.cn

Hao Fan, Bioinformatics Institute (BII), Agency for Science, Technology and Research (A*STAR), Singapore138671, Singapore.
E-mail: fanh@bii.a-star.edu.sg

Abstract

Background & Aims: SLC25A47 was initially identified as a mitochondrial HCC-downregulated carrier protein, but its physiological functions and transport substrates are unknown. We aimed to investigate the physiological role of SLC25A47 in hepatic metabolism.

Approach & Results: In the treatment of hepatocytes with metformin, we found that metformin can transcriptionally activate the expression of *Slc25a47*, which is required for AMP-activated protein kinase α (AMPKα) phosphorylation. *Slc25a47*-deficient mice had increased hepatic lipid content, triglycerides, and cholesterol levels, and we found that *Slc25a47* deficiency suppressed AMPKα phosphorylation and led to an increased accumulation of nuclear SREBPs, with elevated fatty acid and cholesterol

Abbreviations: AMPKα, AMP-activated protein kinase α; CHO, cholesterol; DAG, diglycerides; DEN, diethylnitrosamine; GEPIA, gene expression profiling interactive analysis; HFD, high-fat-diet; IHC, immunohistochemical; KO, knockout; mTOR, mammalian target of rapamycin; ORO, Oil Red O; SIRT3, sirtuin 3; SREBPs, sterol regulatory element binding proteins; TAG, triglycerides; TEM, transmission electron microscopy; WT, wildtype.

Supplemental Digital Content is available for this article. Direct URL citations are provided in the HTML and PDF versions of this article on the journal's website, www.hepjournal.com.

biosynthetic activities. Conversely, when *Slc25a47* was overexpressed in mouse liver, AMPKα was activated and resulted in the inhibition of lipogenesis. Moreover, using a diethylnitrosamine-induced mouse HCC model, we found that the deletion of *Slc25a47* promoted HCC tumorigenesis and development through the activated mammalian target of rapamycin cascade. Employing homology modeling of SLC25A47 and virtual screening of the human metabolome database, we demonstrated that NAD^+ was an endogenous substrate for SLC25A47, and the activity of NAD^+-dependent sirtuin 3 declined in *Slc25a47*-deficient mice, followed by inactivation of AMPKα.

Conclusions: Our findings reveal that SLC25A47, a hepatocyte-specific mitochondrial NAD^+ transporter, is one of the pharmacological targets of metformin and regulates lipid homeostasis through AMPKα, and may serve as a potential drug target for treating NAFLD and HCC.

INTRODUCTION

NAFLD has emerged as the most prevalent liver disease in the world and represents an increased risk factor for type 2 diabetes, NASH, and HCC, as well as liver failure-related transplantation.[1] Despite the widespread prevalence of NAFLD, currently there are no approved pharmacological therapies to prevent or treat this condition.[2] Metformin, the antihyperglycemic agent, and several other experimental compounds have been shown to improve NAFLD in preclinical animal models through increasing the activity of the cellular energy sensor AMP-activated protein kinase α (AMPKα).[2] Metformin reduces liver lipid content by promoting AMPKα phosphorylation of acetyl-CoA carboxylase, which in turn inhibits lipid synthesis, leading to decreased diglyceride and triglyceride (TAG) levels in the liver.[3,4] Developing AMPKα activators, which could potentially suppress *de novo* lipogenesis therefore is a promising approach to target and alleviate NAFLD.

Most AMPKα activators suppress mitochondrial respiration to activate AMPKα,[5] indicating that their pharmacological effects are closely linked to the mitochondria protein function. The SLC25 family (SLC25) comprises at least 53 members and is one of the largest solute carrier protein families involved in the transporter of various metabolites, most of which are expressed in the mitochondria. The SLC25 transporters act as "metabolic gates" involved in transporting essential nutrients and metabolites in the mitochondria.[6] Importantly, multiple SLC transporters have been identified as drug targets for many diseases.[6] Currently, some substrates of the SLC25 family members have been identified, including NAD^+, pyrimidine nucleotide, and amino acids.[7–9] However, there are more than 15 family members whose substrate specificities are unknown. SLC25A47, a mitochondrial carrier protein, was initially found at aberrantly low levels in the tumors of patients with HCC compared to paired noncancerous liver tissue.[10] Recent studies have found that the *Slc25a47*-deficient mice exhibit liver fibrosis characteristics.[11] In addition, SLC25A47 expression was increased in a rat NAFLD model and in steatotic-L02 and HepG2 cells,[12] indicating that SLC25A47 may be involved in lipid metabolism. However, its physiological function and substrate(s) remain unknown.

Here, we investigated the physiological functions and potential substrates of SLC25A47 in the liver. We found that metformin can transcriptionally activate the expression of *Slc25a47,* while its ability to activate AMPKα was weakened due to *Slc25a47* deficiency. That is, AMPKα regulates lipid metabolism homeostasis through SREBPs. Subsequently, *Slc25a47* knockout, overexpression, and DEN-induced HCC mouse models were employed to dissect the molecular mechanism of SLC25A47 in regulating lipid metabolism and HCC development. Furthermore, we constructed a homology model for the human SLC25A47 and performed a virtual screening of human metabolites to identify its putative substates. Finally, NAD^+, identified through virtual screening, was validated as a substrate of SLC25A47 by uptake experiments. Mechanistically, SLC25A47 regulated SIRT3 protein activity through NAD^+ level to mediate the activation of AMPKα. Collectively, these findings indicate that SLC25A47 is a hepatic mitochondrial NAD^+ transporter that regulates lipid metabolism through the SIRT3-AMPKα-SREBPs pathway.

METHODS

Cell culture

HEK293 cells were obtained from ThermoFisher Scientific (Massachusetts, USA). L02, HepG2, Huh7, and Hela cells were obtained from the Chinese Academy of Science

(Shanghai, China). Primary hepatocytes were isolated from adult mice according to Chen's protocol.[13] All cells were cultured in a cell incubator at 37°C with 5% CO2.

Animals

Slc25a47-KO mice were generated using the CRISPR/Cas9 technology according to the protocol.[14] The *Slc25a47*-KO heterozygotes were backcrossed with C57BL/6J mice for at least 8 generations and then used for subsequent breeding and mating. The *Leptin*-deficient heterozygous (*ob*/+) mice were selected to mate with *Slc25a47*-KO mice to obtain *ob/ob* (WT) and *ob/ob* (*Slc25a47*-KO) mice after several generations. For the *Slc25a47*-overexpressing mice, the adenoviruses were delivered to the C57BL/6J mice by tail vein injection. The C57BL/6J mice were purchased from the Laboratory Animal Research Center of Tsinghua University (Beijing, China). All mice were housed in an animal care facility at Tsinghua University under controlled conditions of temperature (22 ± 2 °C) and relative humidity (50 ± 20%), with a 12-hour light/dark cycle with free access to food and water. All animal experiments described were approved by the Institutional Animal Care and Use Committee (IACUC) of Tsinghua University. All animal procedures were consistent with the ARRIVE (Animals in Research: Reporting In Vivo Experiments) guidelines.

Human tissue samples

The paraffin-embedded HCC ($n = 3$) samples used were confirmed by pathological examination at the Beijing Tsinghua Changgung Hospital (Beijing, China). This study was approved by the Ethics Committee of Beijing Tsinghua Chagngung Hospital, and informed consent was obtained before the surgery. The study conforms to the principles outlined in the Declaration of Helsinki. The clinical samples information is summarized in Supplementary Table S1 http://links.lww.com/HEP/D371.

Statistical analysis

Statistical analysis was performed using GraphPad Prism 8 software. Data are expressed as mean ± SEM. Comparisons between groups were performed with a 2-tailed unpaired *t*-test, and the comparison for 3 or more groups was performed with 2-way ANOVA followed by Tukey's multiple comparison test. Statistical significance was calculated and indicated (*$p < 0.05$, **$p < 0.01$, ***$p < 0.001$, and ****$p < 0.0001$).

A detailed description of materials and methods is supplied as Supporting Material.

RESULTS

Metformin regulates *Slc25a47*-mediated AMPKα activation

To investigate the mechanism of metformin on hepatic glucose and lipid metabolism, we performed RNA sequencing analysis on the primary hepatocytes of mice with and without 500 μM metformin treatment. We found that metformin treatment altered the expression of 129 SLC genes and induced a significant increase in the *Slc25a47* expression level (Figure 1A). Similarly, real-time quantitative PCR (qPCR) results demonstrated that the *Slc25a47* expression in metformin-treated hepatocytes was ~3.1-fold higher than in the control without metformin treatment (Figure 1B). In addition, the dual-luciferase reporter assays showed that metformin enhanced SLC25A47 promoter activity in HepG2 and Huh7 cells (Figure 1C).

Expression of *Slc25a47* was found to be highly upregulated only in hepatocytes by single-cell sequencing analysis and expression profiling (Figure 1D and Supplementary Figure 1A, B, Supplemental Digital Content 1, http://links.lww.com/HEP/D370), and RNA sequencing analysis of mouse liver tissues revealed that *Slc25a47* was the most highly expressed gene among SLC transporters (Supplementary Figure 1C, Supplemental Digital Content 1, http://links.lww.com/HEP/D370). In addition, *Slc25a47* was localized to the outer and inner mitochondrial membranes (Supplementary Figure 1D, E, Supplemental Digital Content 1, http://links.lww.com/HEP/D370). These findings demonstrate that *Slc25a47* is a gene specifically expressed in the mitochondria of hepatocytes.

To verify the roles of SLC2547 in the action of metformin, we used metformin to treat primary hepatocytes isolated from the *Slc25a47*-knockout (KO) mice and their wildtype (WT) littermates (generated using CRISPR/Cas9, Supplementary Figure 1F-H, Supplemental Digital Content 1, http://links.lww.com/HEP/D370), to detect AMPKα phosphorylation. Herein the deletion of *Slc25a47* resulted in significantly lower phosphorylation of AMPKα compared to that in hepatocytes from the WT mice (Figure 1E). We also found that the inhibition of *glucose-6-phosphatase catalytic subunit* by metformin was significantly reduced in hepatocytes from the *Slc25a47*-KO mice compared to that in hepatocytes from the WT mice (Figure 1F). These results indicate that SLC25A47 plays an essential role in the activation of AMPKα and the pharmacological effects of metformin in the liver.

Slc25a47 regulates the synthesis of triglycerides and cholesterol by mediating AMPKα activity

To further investigate the physiological roles of Slc25a47, we established a methionine-choline-deficient

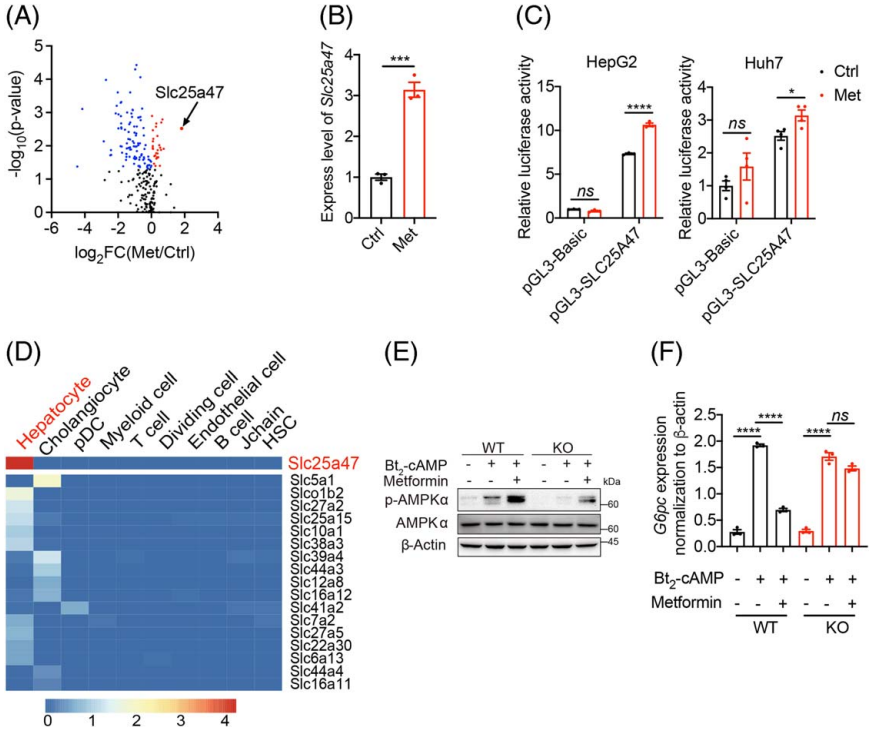

FIGURE 1 Metformin increases the expression of *Slc25a47*. (A) RNA-sequencing analysis volcano plot of metformin regulation of multiple SLC family proteins. (B) Relative mRNA of *Slc25a47* in the primary hepatocytes treated with and without metformin (500 μM) for 6 hours ($n = 3$). (C) Activation of SLC25A47 promoter in HepG2 and Huh7 cells by metformin (HepG2 $n = 3$; Huh7 $n = 4$). (D) Single-cell sequencing analysis of the expression of *Slc25a47* in a different type of mouse liver cells. (E) Immunoblots of AMPKα in hepatocytes of WT and *Slc25a47*-KO mice treated with and without metformin (500 μM) for 6 hours. (F) Inhibitory effect on *glucose-6-phosphatase catalytic subunit* after metformin treatment in primary hepatocytes of WT and *Slc25a47*-KO mice ($n = 3$). Ctrl, Control; Met, Metformin. Data are presented as mean ± SEM. *$p < 0.05$, ***$p < 0.001$,****$p < 0.0001$, *ns*, not significant. Abbrevations: KO, knockout; WT, wildtype.

diet-induced and a high-fat-diet-induced NAFLD model. H&E staining of NAFLD mice liver sections showed that the *Slc25a47*-KO mice had significantly increased hepatic steatosis compared with the WT littermates (Supplementary Figure 2A, Supplemental Digital Content 1, http://links.lww.com/HEP/D370).

In addition to the NAFLD models established by diet induction, we also mated the *Slc25a47*-KO mice with the *leptin*-deficient mice, a genetic NAFLD model, to obtain *Slc25a47* and *leptin* double knockout (*ob/ob* [KO]) mice. We first analyzed the body weight of the *ob/ob* (*Slc25a47*-KO) mice and *ob/ob* (WT) littermates from 4 to 12 weeks of age. The results showed that *ob/ob* (*Slc25a47*-KO) mice were consistently heavier than *ob/ob* (WT) mice (Supplementary Figure 2B, Supplemental Digital Content 1, http://links.lww.com/HEP/D370). The livers and epididymal white adipose tissue (eWAT) of the *ob/ob* (*Slc25a47*-KO) mice were increased by 34.9% and 58.34%, respectively, compared to that of the *ob/ob* (WT) mice at 12 weeks of age (Figure 2A and Supplementary Figure 2C, Supplemental Digital Content 1, http://links.lww.com/HEP/D370). The TAG and cholesterol (CHO) contents in the serum of the *ob/ob* (*Slc25a47*-KO) mice were increased by 24.9% and 35.1%, and in the liver, were increased by 22.1% and 29.7%, respectively, compared to that of the *ob/ob* (WT) mice (Figure 2B). The HDL, LDL, and LDL/HDL content in the serum of the *ob/ob* (*Slc25a47*- KO) mice was also significantly higher than that of the *ob/ob* (WT) mice (Supplementary Figure 2D, Supplemental Digital Content 1, http://links.lww.com/HEP/D370). In the liver tissues, H&E staining, Oil Red O (ORO) staining, and transmission electron microscopy (TEM) revealed significantly increased lipid accumulation in the *ob/ob* (*Slc25a47*-KO) mice with respect to *ob/ob* (WT) mice (Figure 2C and Supplementary Figure 2E, Supplemental Digital Content 1, http://links.lww.com/HEP/D370). Lipidomics analysis of liver extracts by mass spectrometry confirmed the elevated accumulation of TAG and CHO in the *ob/ob* (*Slc25a47*-KO) livers and further revealed increases in diglyceride, TAG, free fatty acids, CHO, and cholesterol esters (Figure 2D).

We performed RNA sequencing by extracting RNA from liver tissues of the *ob/ob* (WT) and the *ob/ob* (*Slc25a47*-KO) mice. Genes related to fatty acid and cholesterol synthesis pathways, including *fatty acid synthase* and *3-hydroxy-3-methylglutaryl-CoA reductase* were increased in the liver of the *ob/ob* (*Slc25a47*-KO) mice with respect to *ob/ob* (WT) mice. In addition, the proprotein convertase subtilisin/kexin type 9, which competitively binds the LDL receptor (LDLR) and reduces the liver's ability to clear LDL-C from the blood,

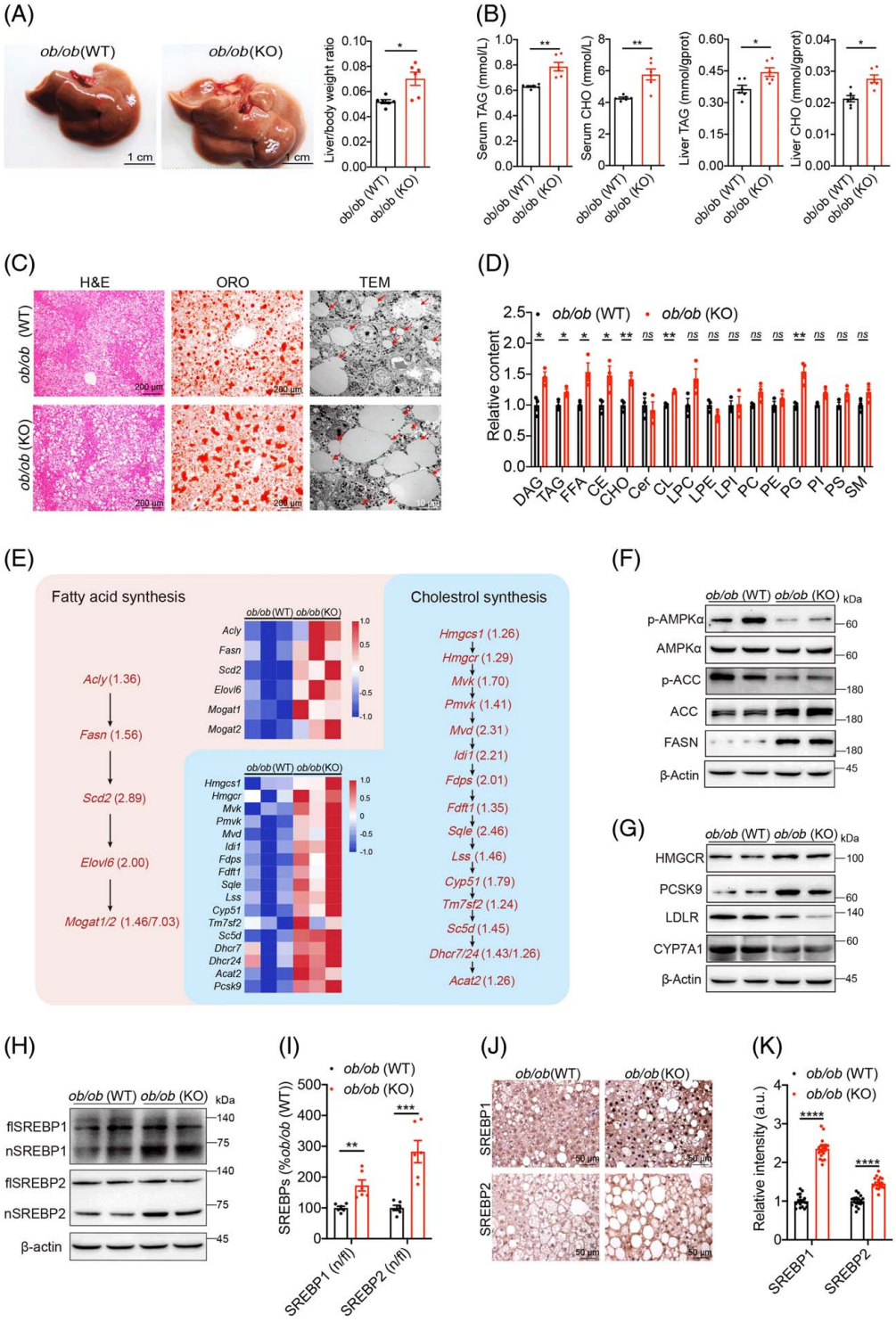

FIGURE 2 *Slc25a47*-deficiency disrupts liver lipid metabolism homeostasis by increasing fatty acid and cholesterol biosynthesis. (A) The liver appearance and liver index of 12-week-old *ob/ob* (WT) and *ob/ob* (*Slc25a47*-KO) mice ($n = 6$). (B) TAG and CHO contents of serum and liver from 12-week-old *ob/ob* (WT) and *ob/ob* (*Slc25a47*-KO) mice ($n = 6$). (C) Liver H&E staining, ORO staining, and TEM of 12-week-old *ob/ob* (WT) and *ob/ob* (*Slc25a47*-KO) mice. (D) Lipidomic analysis of hepatic lipids from *ob/ob* (WT) and *ob/ob* (*Slc25a47*-KO) mice ($n = 3$). (E) Activation of fatty acid and cholesterol biosynthesis pathways by *Slc25a47* knockout ($n = 3$). Immunoblots of fatty acid (F) and cholesterol (G) metabolism pathway in the liver of *ob/ob* (WT) and *ob/ob.* (*Slc25a47*-KO) mice. Immunoblots (H) and its quantitative analysis (I) of full length (fl-) and nuclear (n-) SREBPs expression in the liver of *ob/ob* (WT) and *ob/ob* (*Slc25a47*-KO) mice. IHC staining (J) and its quantitative analysis (K) of SREBPs expression in the liver of *ob/ob* (WT) and *ob/ob* (*Slc25a47*-KO) mice. Data are presented as mean ± SEM. $^{*}p < 0.05$, $^{**}p < 0.01$, $^{***}p < 0.001$, $^{****}p < 0.0001$. Abbreviations: CHO, cholesterol; IHC, immunohistochemical; KO, knockout; ORO, Oil Red O; SREBPs, sterol regulatory element binding proteins; TAG, triglycerides; transmission electron microscopy; TEM,transmission electron microscopy; WT, wildtype.

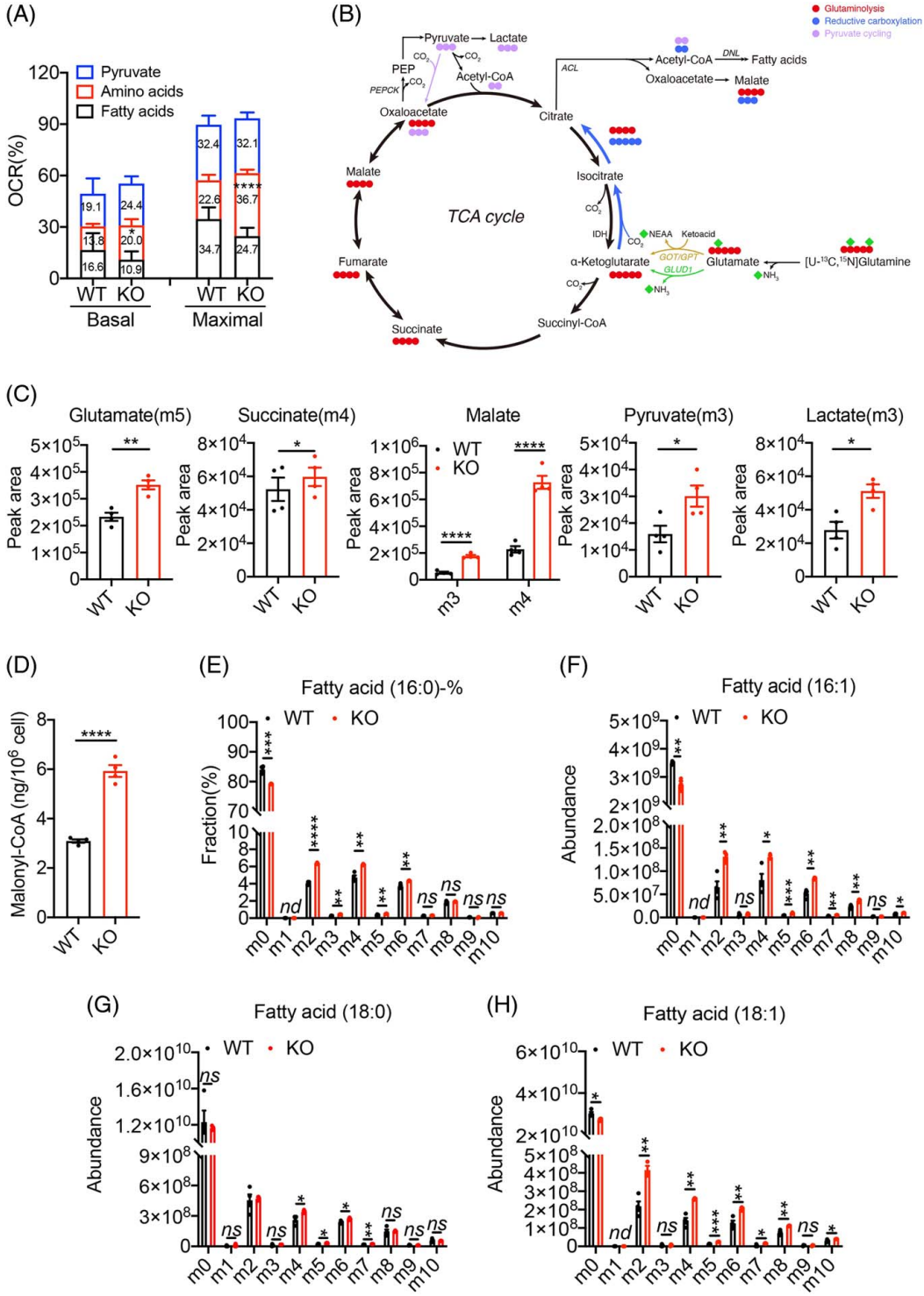

FIGURE 3 *Slc25a47* deficiency promotes lipid synthesis. (A) The fractional contribution of pyruvate, amino acid, and fatty acid in basal and maximal mitochondrial respiration of primary hepatocytes of WT and *Slc25a47*-KO mice calculated by the inhibition percentage of UK5099, AOA, and Etomoxir, respectively ($n = 5$). (B) Scheme outlining the path of ^{13}C-Glutamine in the TCA cycle of primary hepatocytes. (C) Accumulation kinetics of ^{13}C isotope-labeled TCA cycle intermediates during the course of ^{13}C-Glutamine tracing ($n = 4$). (D) Malonyl-CoA content in primary hepatocytes of the WT and *Slc25a47*-KO mice ($n = 4$). (E) Fractional abundance of triglyceride palmitate (C16:0 FA) isotopomers in primary hepatocytes from the WT and *Slc25a47*-KO mice traced with 10 mM ^{13}C-Glutamine (WT $n = 4$; *Slc25a47*-KO $n = 3$). (F-G) Abundance of the most enriched triglyceride FA (C16:1, C18:0, C18:1) isotopomers in primary hepatocytes from WT and *Slc25a47*-KO mice traced with 10 mM ^{13}C-Glutamine (WT $n = 4$; *Slc25a47*-KO $n = 3$). Data are presented as mean ± SEM. *nd* means not detected. $^*p < 0.05$, $^{**}p < 0.01$, $^{***}p < 0.001$, $^{****}p < 0.0001$, *ns*, not significant. Abbreviations: AOA, aminooxyacetate; KO, knockout; WT, wildtype.

was increased by 225.5% in the liver of the *ob/ob* (*Slc25a47*-KO) mice with respect to *ob/ob* (WT) mice (Figure 2E).

Immunoblot analysis showed that AMPKα phosphorylation was significantly reduced in the liver of the *ob/ob* (*Slc25a47*-KO) mice with respect to *ob/ob* (WT) mice, resulting in the elevated protein levels of key lipogenic enzymes, such as acetyl-CoA carboxylase and *fatty acid synthase*, in the liver of the *ob/ob* (*Slc25a47*-KO) mice (Figure 2F). Similarly, compared to the *ob/ob* (WT) mice, the protein levels of cholesterol synthesis-related enzymes, such as *3-hydroxy-3-methylglutaryl-CoA reductase*, were increased. In addition, proprotein convertase subtilisin/kexin type 9 was significantly increased, and correspondingly, the protein level of its ligand LDL receptor was decreased in the *ob/ob* (*Slc25a47*-KO) mice, as well as the cholesterol clearance-related enzyme cytochrome P450 family 7 subfamily A member 1 (Figure 2G).

We further analyzed the protein levels of SREBP1 and SREBP2, which are important regulators of fatty acid and cholesterol metabolism. We detected that the nuclear levels of SREBP1 and SREBP2 were increased by 72.8% and 182.7% in the *ob/ob* (*Slc25a47*- KO) mice, respectively, with respect to *ob/ob* (WT) mice (Figure 2H, I), indicating that *Slc25a47* knockout can enhance SREBP1 and SREBP2 cleavage and activation. Similarly, hepatic SREBP1 and SREBP2 activation in *Slc25a47* knockout was confirmed by immunohistochemical (IHC) staining in liver sections and immunofluorescence staining in primary hepatocytes (Figure 2J, K and Supplementary Figure 2F, Supplemental Digital Content 1, http://links.lww.com/HEP/D370). Collectively, these data suggested that SLC25A47 regulated hepatic lipid homeostasis though the AMPKα-SREBPs signaling pathway.

Slc25a47-KO hepatocytes mainly utilize amino acids to provide energy for lipid synthesis

We found that there were more lipid droplets in primary hepatocytes from the *Slc25a47*- KO mice than in those from the WT littermates (Supplementary Figure 3A, B, Supplemental Digital Content 1, http://links.lww.com/HEP/D370), and the TAG and CHO contents in *Slc25a47*-KO hepatocytes were increased by 48.6% and 104.1%, respectively, compared to WT hepatocytes (Supplementary Figure 3C, Supplemental Digital Content 1, http://links.lww.com/HEP/D370). During the knockdown of AMPKα in WT and *Slc25a47*-KO hepatocytes, respectively, the TAG and CHO contents were significantly increased compared with WT and *Slc25a47*-KO hepatocytes (Supplementary Figure 3D, E, Supplemental Digital Content 1, http://links.lww.com/HEP/D370). Therefore, we used hepatocytes to investigate the promotion of lipid synthesis by *Slc25a47* deficiency.

To measure the contributions of various substrates to the TCA cycle, we compared mitochondrial respiration in the presence or absence of fatty acid transporters (etomoxir [ETO]), transaminases (aminooxyacetate [AOA]), and pyruvate transporters (UK5099) (Liao et al., unpublished data, 2021) inhibitors. We found that the contribution of amino acids to mitochondrial respiration was higher in *Slc25a47*-KO hepatocytes than in WT hepatocytes (Figure 3A and Supplementary Figure 3F, Supplemental Digital Content 1, http://links.lww.com/HEP/D370). Therefore, with glutamine as the representative amino acid, as well as glucose, we applied the OpenMebius flux model (Liao et al., unpublished data, 2021) to investigate the contribution of glucose and amino acids to the TCA cycle (Figure 3B and Supplementary Figure 3G, Supplemental Digital Content 1, http://links.lww.com/HEP/D370). The results demonstrated that the utilization efficiency of glucose in *Slc25a47*-KO hepatocytes did not differ from that in WT hepatocytes (Supplementary Figure 3H, Supplemental Digital Content 1, http://links.lww.com/HEP/D370), whereas the utilization efficiency of glutamine in *Slc25a47*-KO hepatocytes was higher than that in WT hepatocytes (Figure 3C). Moreover, the content of malonyl-CoA in *Slc25a47*-KO hepatocytes was almost twice that of WT hepatocytes as measured by ELISA (Figure 3D). These results indicate that *Slc25a47*-KO mainly utilizes amino acids to provide energy for fatty acid synthesis.

Additionally, we investigated fatty acid synthesis from amino acids in the *Slc25a47* knockout by measuring the efficiency of glutamine metabolic flux to fatty acid synthesis. Glutamine-derived ^{13}C was incorporated into palmitate in the *Slc25a47*-KO hepatocytes much more efficiently than in the WT hepatocytes (Figure 3E). Immediate elongation and desaturation products of palmitate, including palmitoleate (C16:1), stearate (C18:0), and oleate (C18:1), were adequately labeled, and the labeling rate in the *Slc25a47*-KO hepatocytes was higher than that of the WT hepatocytes, suggesting increased desaturation in the *Slc25a47*-KO hepatocytes than in the WT hepatocytes (Figure 3F-H). Therefore, we concluded that amino acids are essential substances for fatty acid synthesis in the *Slc25a47*-KO hepatocytes.

Overexpression of *Slc25a47* inhibits lipid accumulation

To examine whether overexpression of *Slc25a47* would reduce hepatic lipid accumulation, Ad-*Slc25a47* and control Ad-*GFP* adenoviruses were delivered to adult C57BL/6J mice fed with high-fat-diet for 4 weeks through the tail vein. Seven days after the injection of

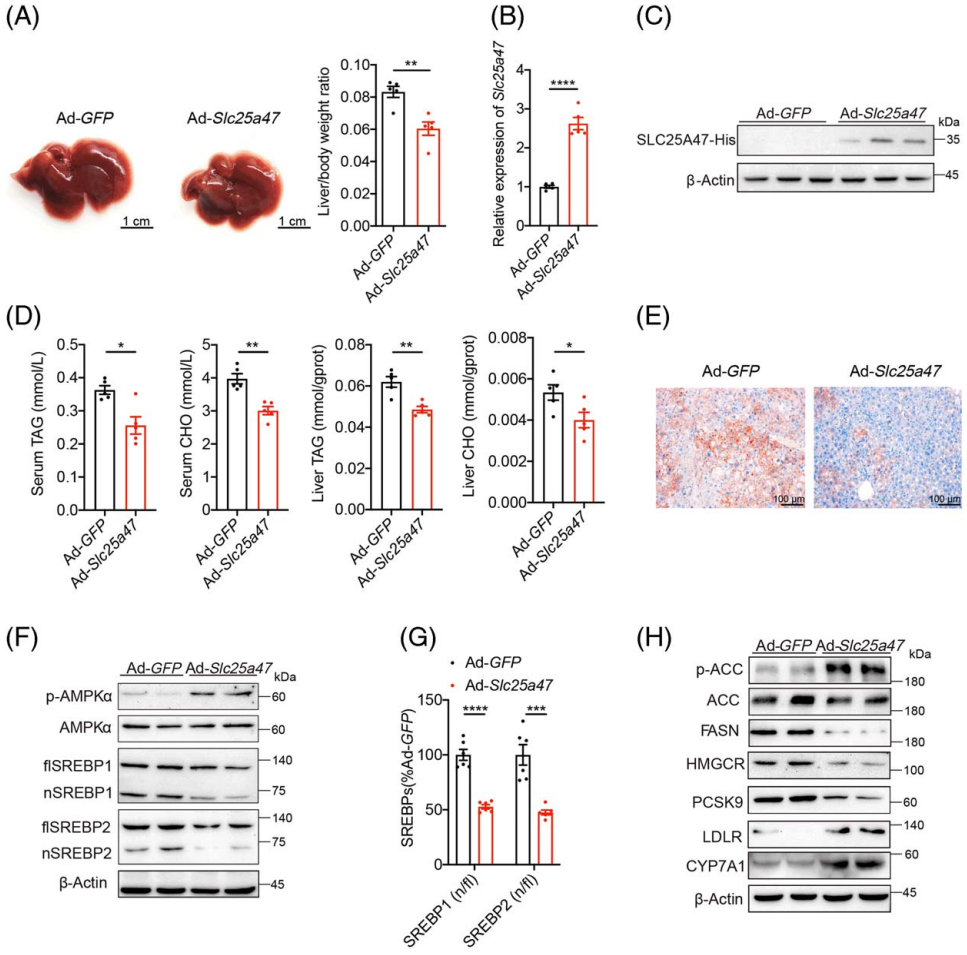

FIGURE 4 Overexpression of *Slc25a47* inhibits lipid accumulation. (A) The liver appearance and liver index of Ad-*GFP* and Ad-*Slc25a47* mice ($n = 5$). (B) *Slc25a47* expression in the liver of Ad-*GFP* and Ad-*Slc25a47* mice ($n = 5$). (C) Immunoblots of SLC25A47-His in the liver of Ad-*GFP* and Ad-*Slc25a47* mice. (D) TAG and CHO contents in the serum and liver of Ad-*GFP* and Ad-*Slc25a47* mice ($n = 5$). (E) ORO staining in liver tissues of Ad-*GFP* and Ad-*Slc25a47* mice. (F) Immunoblots of AMPKα and SREBPs in the liver of Ad-*GFP* and Ad-*Slc25a47* mice. (G) Quantitative analysis of immunoblotting for full length (fl-) and nuclear (n-) SREBPs expression in the liver of Ad-*GFP* and Ad- *Slc25a47* mice. (H) Immunoblots of fatty acid and the cholesterol metabolism pathway in the liver of Ad-*GFP* and Ad-*Slc25a47* mice. Data are presented as mean ± SEM. $^{*}p < 0.05$, $^{**}p < 0.01$, $^{***}p < 0.001$, $^{****}p < 0.0001$. Abbreviations: AMPKα, AMP-activated protein kinase α; CHO, cholesterol; ORO, Oil Red O; SREBPs, sterol regulatory element binding proteins; TAG, triglycerides.

control Ad-*GFP* and Ad-*Slc25a47*, liver tissue and serum were harvested to determine whether the overexpression of *Slc25a47* could inhibit lipid accumulation. There was no significant difference in body weight between the 2 groups of mice (Supplementary Figure 4A, Supplemental Digital Content 1, http://links.lww.com/HEP/D370), but the livers from the Ad-*Slc25a47* mice were 27.4% smaller than from the Ad-*GFP* mice (Figure 4A). The *Slc25a47* mRNA expression level in the livers of the Ad-*Slc25a47* mice showed a strong increase (1.62-fold) compared to that of the Ad-*GFP* mice (Figure 4B). Immunoblot analysis showed that the SLC25A47-His-tag protein level in the livers of the Ad-*Slc25a47* mice also increased compared to that of the Ad-*GFP* mice (Figure 4C). Therefore, this method was shown to induce the specific overexpression of *Slc25a47* in the liver.

Subsequently, the TAG and CHO contents in the serum and liver tissues from the Ad-*GFP* and Ad-*Slc25a47* mice were examined. Compared with the Ad-*GFP* mice, the contents of TAG and CHO in the serum of the Ad-*Slc25a47* mice were decreased by 29.5%, and 24.3%, and in the liver tissue were decreased by 21.6% and 25.0%, respectively (Figure 4D). Oil Red O staining of the liver tissues also confirmed that hepatic ectopic expression of *Slc25a47* alleviated hepatic steatosis in mice (Figure 4E). In addition, the hepatic overexpression of *Slc25a47* in the *ob/ob* (WT) and *ob/ob* (*Slc25a47*-KO) mice also proved that it can reduce the hepatic steatosis in mice (Supplementary Figure 4B, C, Supplemental Digital Content 1, http://links.lww.com/HEP/D370). Similarly, the TAG and CHO contents in Ad-*Slc25a47* hepatocytes were also significantly reduced compared to Ad-*GFP* hepatocytes (Supplementary Figure 4D, E,

Supplemental Digital Content 1, http://links.lww.com/HEP/D370).

Since we speculated that SLC25A47 regulates lipid metabolism by regulating the AMPKα-SREBPs pathway, we also examined the level of AMPKα phosphorylation by immunoblotting. We found that AMPKα phosphorylation in the liver of Ad-*Slc25a47* mice was significantly activated compared to Ad-*GFP* mice (Figure 4F). Compared with Ad-*GFP* mice, the proportion of activated SREBP1 and SREBP2 in the liver nuclei of Ad-*Slc25a47* mice decreased by 47.3% and 52.4%, respectively (Figure 4F, G). Our results clearly show that overexpression of *Slc25a47* resulted in the activation of the AMPKα-SREBPs pathway, which in turn significantly decreased the expression of enzymes related to fatty acid and cholesterol synthesis in the liver, thereby reducing the lipid content in the liver (Figure 4H).

SLC25A47 mediates HCC tumorigenesis and development by regulating lipid metabolism

Since SLC25A47 was originally identified as an HCC-downregulated protein, we screened the Gene Expression Profiling Interactive Analysis (GEPIA) database and found that the expression of SLC25A47 at the mRNA level was significantly reduced in HCC tumors compared with paracancerous tissues (Figure 5A). Patients with lower SLC25A47 protein expression in the liver had a faster recurrence and lower 5-year survival rates (Figure 5B). The IHC staining results of liver tissue from 3 HCC patients also showed that the protein level of SLC25A47 was significantly lower than that in the paracancerous tissues (Figure 5C).

We observed no visible tumors in the livers of 20-month-old WT mice (fed a normal chow diet), but detected liver tumors in 77.8% of the age-matched *Slc25a47*-KO mice (Supplementary Figure 5A, B, Supplemental Digital Content 1, http://links.lww.com/HEP/D370). H&E and Oil Red O staining showed that lipid accumulation in the liver of *Slc25a47*-KO mice occurred predominantly in the tumor (Supplementary Figure 5C, Supplemental Digital Content 1, http://links.lww.com/HEP/D370). IHC staining of Ki67, a marker of cellular proliferative activity, demonstrated marked tumor cell proliferation in the livers of *Slc25a47*-KO mice (Supplementary Figure 5C, Supplemental Digital Content 1, http://links.lww.com/HEP/D370).

To further investigate the role of SLC25A47 in HCC tumorigenesis, we compared HCC development in WT and *Slc25a47*-KO mice by DEN treatment. DEN is a widely used hepatic carcinogen used in HCC studies, functioning as a potent trigger for chromatin instability. We injected DEN intraperitoneally into 2-week-old WT and *Slc25a47*-KO mice and sacrificed them at the 40th week. Compared with the WT HCC mice, the *Slc25a47*-KO HCC mice had a mortality rate of ~40% (Figure 5D). Although there was no significant difference in body weight between the 2 groups of mice (Figure 5E), the *Slc25a47*-KO HCC mice had a 97.5% increase in the liver index compared to WT HCC mice, and the number of tumor nodules was 2.41-fold higher than that of WT HCC mice (Figure 5F). IHC and immunoblot analysis suggested that compared with WT HCC mice, *Slc25a47*-KO HCC mice had increased tumor cell proliferation and multiple upregulated multiple fibrotic factors such as Collagen I, FN1, and α-SMA (Figure 5G, H). These results indicated that *Slc25a47* knockout in the liver promoted the pathological process of DEN-induced HCC. We found that there was significant lipid accumulation in the tumor nodules of *Slc25a47*-KO mice (Figure 5I), and immunoblotting also suggested that SLC25A47 mediated HCC tumorigenesis and development by regulating lipid metabolism (Figure 5J, K). Moreover, we found that SLC25A47 deficiency activated the mammalian target of the rapamycin (mTOR) signaling pathway (Figure 5L, M and Supplementary Figure 5D, Supplemental Digital Content 1, http://links.lww.com/HEP/D370). Furthermore, i.p. injection of mTOR inhibitor rapamycin (2 mg/kg)[15,16] every other day in the last 8 weeks of DEN-induced HCC mice could significantly alleviate the HCC tumorigenesis (Supplementary Figure 5E, Supplemental Digital Content 1, http://links.lww.com/HEP/D370). Therefore, SLC25A47 mediates HCC tumorigenesis by regulating the AMPKα-mTOR-SREBPs signaling pathway.

SLC25A47 is an NAD$^+$ transporter

SLC25A47 is considered to be an amino acid transporter based on phylogenetic tree analysis using ClustalW multiple-sequence alignment in MEGA5.[17] To discover the transport substrate of SLC25A47, we analyzed the uptake of ^{13}C-labeled amino acids and non-isotopically labeled amino acids by the liver mitochondria of the WT and *Slc25a47*-KO mice and found that *Slc25a47* was not an amino acid transporter (Supplementary Figure 6A, B, Supplemental Digital Content 1, http://links.lww.com/HEP/D370).

To further explore potential transport substrates of SLC25A47, we modelled the 3D structure of the human SLC25A47 protein using Modeller v9.25 based on the bovine SLC25A4 mitochondrial ADP/ATP transporter structure (PDB ID: 1OKC[18]) (Figure 6A [i, ii]). Structure-based sequence analysis of the bovine SLC25A4 transporter and the human SLC25A47 protein showed the presence of 3 SOLCAR repeats, conserved kink-inducing proline residues (P19, P132, and P237 in human SLC25A47) in odd-numbered transmembrane helices, and a cationic motif (RRRMMM in SLC25A4

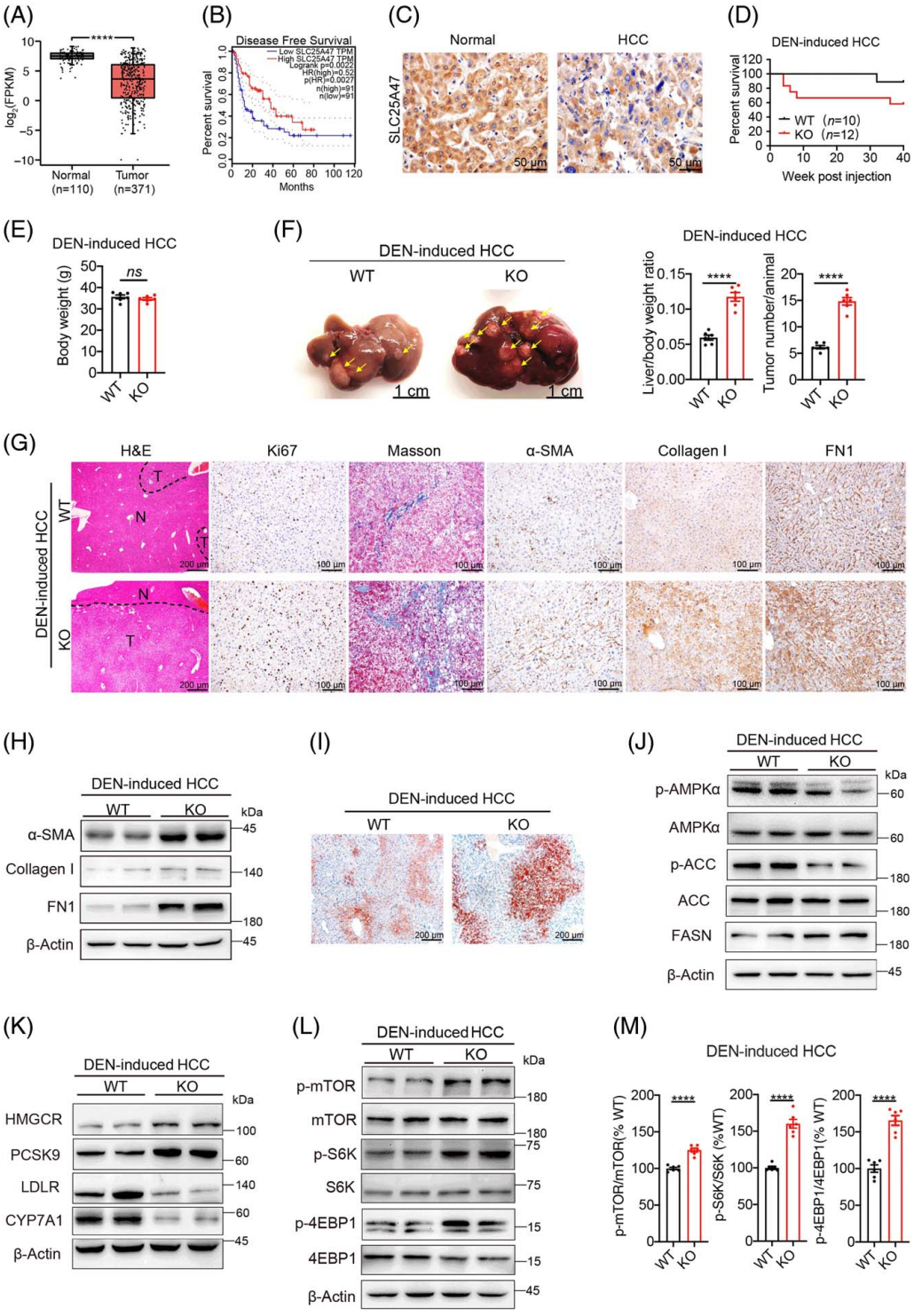

FIGURE 5 SLC25A47 deficiency promotes the pathogenesis of HCC. (A) The expression level of SLC25A47 in HCC samples compared with paracancerous tissues was determined from the GEPIA database (Normal $n = 110$; Tumor $n = 371$). (B) Effect of SLC25A47 expression on the overall survival of HCC patients in the GEPIA database ($n = 91$). (C) IHC staining analysis of the expression of SLC25A47 in HCC tumors and its paracancerous tissues. (D) Survival curve of HCC model induced by DEN treatment in the WT and *Slc25a47*-KO mice (WT $n = 10$; *Slc25a47*-KO $n = 12$). Body weight (E), liver appearance, and liver index (F) of DEN-treatment mice at the end of the 10th month ($n = 6$). (G) H&E, Masson staining, and IHC staining of Ki67, α-SMA, Collagen I, and Fn1 in the liver of WT and *Slc25a47*-KO mice with DEN-treatment. (H) Immunoblots analysis of fibrosis markers in the liver of WT and *Slc25a47*-KO mice with DEN treatment. (I) ORO staining of the liver from WT and *Slc25a47*-KO mice with DEN treatment. (J, K) Immunoblots of AMPKα and its regulated proteins related to fatty acid and cholesterol metabolism pathways in the liver of WT and *Slc25a47*-KO mice with DEN-treatment. (L) Immunoblots of the mTOR pathway in the liver of WT and *Slc25a47*-KO mice with DEN treatment. (M) Quantitative analysis of immunoblotting for mTOR pathway-related proteins in the liver of WT and *Slc25a47*-KO mice with DEN treatment ($n = 6$). Data are presented as mean ± SEM. ****$p < 0.0001$, *ns*, not significant. Abbreviations: DEN, diethylnitrosamine; GEPIA, Gene Expression Profiling Interactive Analysis; IHC, immunohistochemical; KO, knockout; mTOR, mammalian target of rapamycin; ORO, Oil Red O; WT, wildtype.

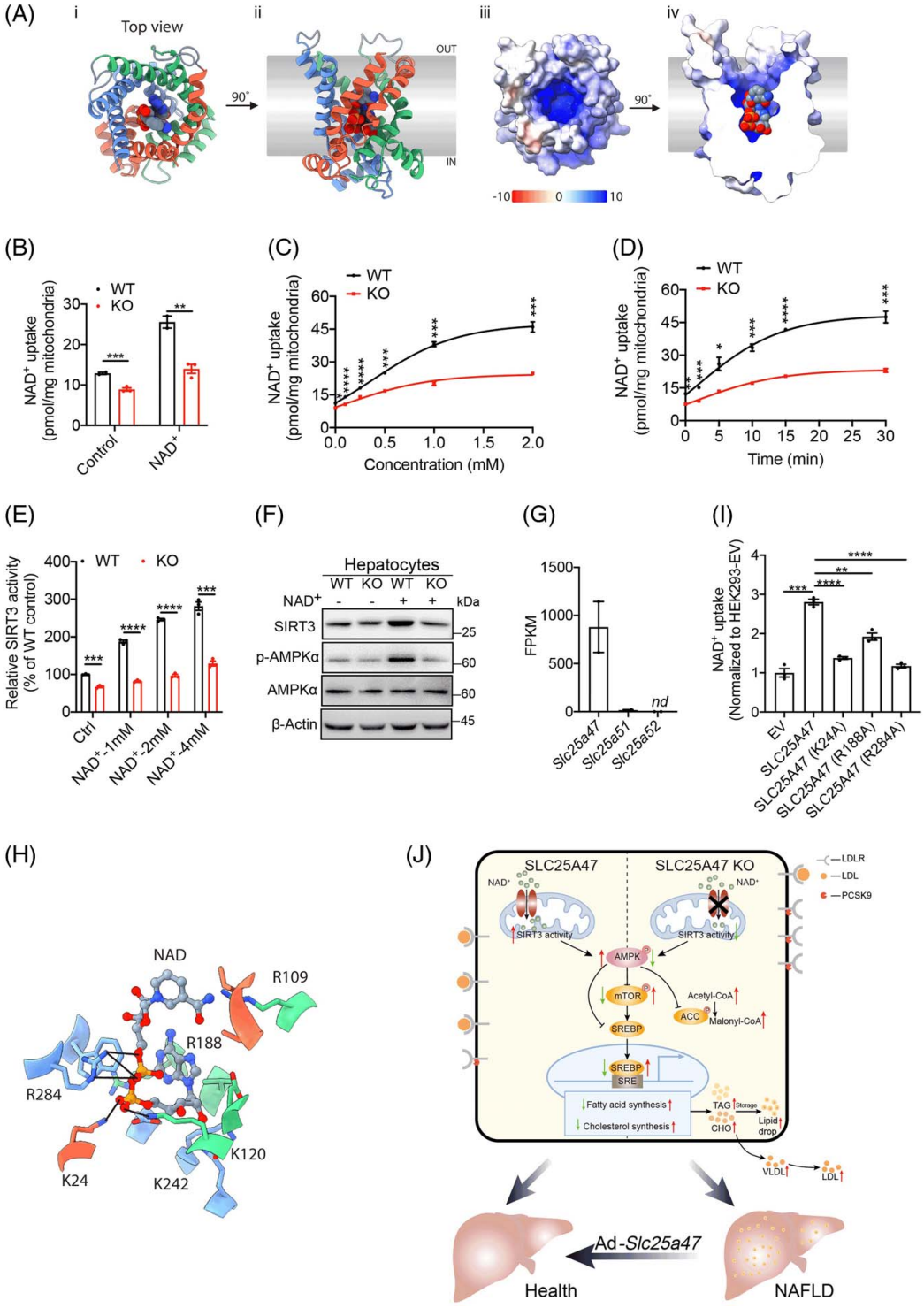

FIGURE 6 SLC25A47 is identified as a mitochondrial NAD^+ transporter. (A) 3D- homology model of human SLC25A47. (B) Uptake of NAD^+ by liver mitochondria of the WT and *Slc25a47*-KO mice ($n = 3$). (C, D) Concentration-response and time-response curves of liver mitochondria from the WT and *Slc25a47*-KO mice to NAD^+ ($n = 3$). (E) SIRT3 activity in liver mitochondria of the WT and *Slc25a47*-KO mice ($n = 3$). (F) Immunoblots of SIRT3, p-AMPKα, and AMPKα in hepatocytes of the WT and *Slc25a47*-KO mice with and without NAD^+ treatment. (G) mRNA expression of *Slc25a47*, *51,* and *52* in mouse liver ($n = 2$). (H) Close-up view of the binding pocket residues surrounding the docked NAD^+ molecule. Potential electrostatic/salt-bridge interactions between cationic residues and the phosphate group of NAD^+ are shown with black lines. (I) Uptake of NAD^+ by EV, SLC25A47, and mutant SLC25A47 in stably transfected HEK293 cell lines ($n = 3$). (J) A proposed model for the role of SLC25A47 in regulating hepatic lipid metabolism. Data are presented as mean ± SEM. nd means not detected. $^*p < 0.05$, $^{**}p < 0.01$, $^{***}p < 0.001$, $^{****}p < 0.0001$. Abbreviations: AMPKα, AMP-activated protein kinase α; KO, knockout; WT, wildtype.

and KSRLQA in human SLC25A47) characteristic of proteins in the mitochondrial carrier family (TC 2.A.29).

Using this homology model of human SLC25A47, we performed a docking-based virtual screening of the Human Metabolome Database and obtained a series of substrate candidates, including NAD^+, acetyl-CoA, adenosine, and flavin adenine dinucleotide (Supplementary Table S2, Supplemental Digital Content 2, http://links.lww.com/HEP/D371). We mapped the electrostatic potential surface of the human SLC25A47 homology model (Figure 6A [iii, iv]) using the Adaptive Poisson- Boltzmann Solver.[19] The electrostatic potential surface map indicated that the interior of the transporter is largely positive, comprising cationic residues Arg and Lys, and thus could favorably interact with the anionic phosphate and aromatic nucleotide groups of NAD^+. We used mouse liver mitochondria to perform uptake experiments on the potential substrates. The results showed that *Slc25a47* knockout reduced the uptake of NAD^+ and acetyl-CoA by 45.9% and 53.6%, respectively, in mouse liver mitochondria. Conversely, there was no significant difference in the uptake of adenosine or flavin adenine dinucleotide compared with WT mouse liver mitochondria (Figure 6B and Supplementary Figure 6C, Supplemental Digital Content 1, http://links.lww.com/HEP/D370).

The NAD^+ uptake assay by mouse liver mitochondria also found that the absorption of NAD^+ by *Slc25a47* was concentration-dependent and time-dependent (Figure 6C, D).

Furthermore, we overexpressed mouse *Slc25a47* in the liver of *Slc25a47* KO mice (KO+Ad-*Slc25a47* mice), then isolated the mitochondria from WT, *Slc25a47* KO, and *Slc25a47* KO+Ad-*Slc25a47* mice and incubated with 1mM NAD^+ for 15 min, and the result showed that the overexpression of *Slc25a47* rescued mitochondrial NAD^+ uptake (Supplementary Figure 6D, Supplemental Digital Content 1, http://links.lww.com/HEP/D370). NAD^+ is a substrate of sirtuins; among the seven known sirtuins, sirtuin 3 (SIRT3) mainly plays an important role in mitochondrial energy metabolism and function, and its activity is controlled by NAD^+ concentration.[20] Therefore, we evaluated the SIRT3 protein activity in mitochondria from WT and *Slc25a47*-KO mice livers and found that as NAD^+ concentration increased, SIRT3 protein activity in *Slc25a47*-KO mice mitochondria decreased with respect to that in WT mice mitochondria (Figure 6E). Additionally, SIRT3 is associated with activation of the AMPKα signaling pathway.[21] Immunoblotting results also showed that NAD^+ could increase the protein expression levels of SIRT3 and phosphorylated AMPKα in hepatocytes of WT mice but had little effect on the protein expression levels of SIRT3 and phosphorylated AMPKα in the hepatocytes of *Slc25a47*-KO mice (Figure 6F). Knockdown SIRT3 in hepatocytes of the WT and *Slc25a47*-KO mice could significantly reduce the expression level of phosphorylated AMPKα (Supplementary Figure 6E, Supplemental Digital Content 1, http://links.lww.com/HEP/D370). Co-immunoprecipitation experiments indicated that there is no direct protein-protein interaction between Slc25a47 and Sirt3 (Supplementary Figure 6F, Supplemental Digital Content 1, http://links.lww.com/HEP/D370). Therefore, we concluded that Slc25a47 modulates the activity of NAD^+-dependent SIRT3 through its substrate NAD^+.

Although studies have reported that the mitochondrial carrier family members SLC25A51/52 are NAD^+ transporters,[22] we observed extremely low expression of *Slc25a51/52* in the liver and hepatocytes (Figure 6G and Supplementary Figure 6G, Supplemental Digital Content 1, http://links.lww.com/HEP/D370), and the exogenous expression of mouse *Slc25a51* in the liver of *Slc25a47*-KO mice could increase mitochondrial NAD^+ uptake (Supplementary Figure 6H, Supplemental Digital Content 1, http://links.lww.com/HEP/D370).

The SLC25A47 homology model clearly showed favorable electrostatic interactions between the phosphate group of the docked NAD^+ molecule and residues K24, K120, and R284 (Figure 6H). Interestingly, residues R188, K242, and R284 in human SLC25A47 are also sequentially and structurally conserved in the recently identified mammalian NAD^+ transporter SLC25A51[22] (R182, K236, and R278). Residue conservation analysis carried out using Consurf[23] also clearly showed a high degree of residue conservation within the central cavity among 150 SLC25A47 sequence homologs, with identity values ranging from 35% to 95% (Supplementary Figure 6I, Supplemental Digital Content 1, http://links.lww.com/HEP/D370). Our data also showed that HEK293 cells with overexpressed SLC25A47 had a 1.81-fold increased uptake of NAD^+ compared to overexpression empty vector (EV, control), whereas NAD^+ uptake levels were greatly reduced in HEK293 cells with overexpressed mutant SLC25A47 (K24A, R188A, and R284A) (Figure 6I), supporting that SLC25A47 functions as a hepatic mitochondrial NAD^+ transporter.

To summarize, the *Slc25a47*-KO reduced the NAD^+ transporter capacity, which in turn brought SIRT3 activity down, thereby inhibiting AMPKα activity and regulating the hepatic lipid metabolism homeostasis through the AMPKα-SREBPs signaling pathway. Consequently, lipid synthesis was promoted, causing the accumulation of lipid droplets in the liver, which ultimately led to the occurrence of NAFLD and HCC (Figure 6J).

DISCUSSION

Metformin has significant benefits in the treatment of T2D and NAFLD,[13,24] but the underlying mechanisms of

action are complex and not fully understood. Metformin treatment can significantly upregulate the expression level of *Slc25a47* and activate AMPKα in hepatocytes, which was greatly reduced in *Slc25a47*-KO, indicating a previously unknown fact that SLC25A47 is involved in metformin's pharmacological action network through the AMPKα activation. Conversely, loss of *Slc25a47* leads to the deactivation of AMPKα and stimulates lipogenic activities regulated by SREBPs.[25] Studies have shown that AMPKα phosphorylation mediates the activities of downstream SREBP1/2 by activating genes involved in triglyceride and cholesterol synthesis.[25] Also, the upregulation of proprotein convertase subtilisin/kexin type 9 accelerates the LDL receptor degradation, which prevents the clearance of plasma LDL-cholesterol.[26] Both TAG and CHO are thereby elevated in the serum and liver of *Slc25a47* deficient mice. We also demonstrate that the loss of *Slc25a47* drives the fatty acid synthesis from amino acids but not glucose, indicating that *Slc25a47* deficiency further increases cellular utilization of glutamine metabolic flux, promoting fatty acid synthesis and lipid accumulation in hepatocytes. Consistently, overexpressing *Slc25a47* in the liver can inhibit the activity of SREBPs by activating AMPKα, thereby suppressing lipid synthesis and achieving the goal of alleviating NAFLD. These findings support that SLC25A47 is an activator of AMPKα phosphorylation, regulating SREBPs to maintain the biosynthesis of fatty acids and cholesterol.

AMPKα can directly phosphorylate multiple components of the mTOR pathway.[27] Activation of mTOR signaling is a critical molecular event in the tumorigenesis in HCC,[28] and mTOR inhibition can effectively delay or treat HCC caused by mTOR overactivation, for which a variety of mTOR inhibitors developed.[29] mTOR regulates the expression of many adipogenesis enzymes through the modulation of transcription factor SREBPs that control lipid synthesis.[30] Increased levels of lipogenesis are an emerging metabolic hallmark of HCC.[31] *Slc25a47* deletion activates the mTOR signaling pathway by inhibiting AMPKα phosphorylation, which in turn promotes SREBPs activities to elevate lipid synthesis facilitating HCC progression. The significant downregulation of *Slc25a47* in patients with HCC may deregulate the mTOR pathway and result in higher activities of lipogenesis to support HCC tumor cell growth.

Several studies have described the phylogenetic tree of human mitochondrial carrier proteins based on sequence similarity and have speculated that SLC25A47 may be an amino acid transporter.[17] We found that the uptake of amino acids by the liver mitochondria in *Slc25a47*-KO mice was not significantly inhibited compared with WT (Supplementary Figure 6A, B, Supplemental Digital Content 1, http://links.lww.com/HEP/D370). Using virtual screening of a library of human metabolites against a predicted human SLC25A47 homology model coupled with *in vitro* uptake studies, we identified that NAD^+ is likely to be an endogenous substrate for SLC25A47. It is possible that there exists other substrates for SLC25A47. Several studies have shown that SLC25A51/52 are the main transporters of NAD^+,[22,32] while the expression of *Slc25a51/52* is much lower than *Slc25a47* or not expressed in the liver (Figure 6G and Supplementary Figure 6G, Supplemental Digital Content 1, http://links.lww.com/HEP/D370), and *Slc25a51/52* are mainly expressed in other tissues. Therefore, SLC25A47 may be the main hepatic mitochondrial NAD^+ transporter. The liver is an important organ for NAD^+ metabolism and is thought to release metabolites such as nicotinamide and possibly control NAD^+ metabolism in other organs.[33] The *Slc25a47* deficiency probably caused the decreased mitochondrial NAD^+ level to promote NAFLD and HCC development. Declined NAD^+ pooling increased hepatic susceptibility to NAFLD and even HCC, whereas increased NAD^+ level tended to prevent NAFLD,[34] suggesting that supplementation of NAD^+ is a beneficial prophylactic or therapeutic approach in NAFLD and HCC.[34]

SIRT3 is a mitochondrial NAD^+-dependent deacetylase that regulates energy metabolism. Studies have shown that SIRT3-deficient mice suffer from fatty acid oxidation disorders,[35] and when fed a high-fat-diet, SIRT3-deficient mice exhibit accelerated development of metabolic syndrome features such as obesity, hyperlipidemia, and steatohepatitis.[36] In contrast, SIRT3 overexpression not only promotes lipid droplet degradation in hepatocytes by activating AMPKα but also inhibits adipogenesis by reducing the expression of stearoyl-CoA desaturase1.[37] Multiple studies have shown that SIRT3 functions by activating AMPKα.[21,37,38] In our study, deletion of Slc*25a47* results in reduced mitochondrial NAD^+ level, which in turn brings the SIRT3 activity down, thereby leading to the inhibition of the AMPKα phosphorylation and upregulation of the activities of mTOR and SREBPs (Figure 6J).

In conclusion, we identified that SLC25A47 is a hepatic NAD^+ transporter regulating hepatic lipogenesis through the SIRT3-AMPKα-SREBPs pathway, which may be an important target for metformin to exert its pharmacological effects. These findings have laid the foundation for developing gene delivery tools or agonists on SLC25A47 for NAFLD and HCC treatments.

AUTHOR CONTRIBUTIONS

Study design: Lili Cheng and Ligong Chen; Performing the experiments: Lili Cheng, Guoqiang Wang, Ziyi Meng, Mengqing Xie, Wenna Chi, Yuming Zhang, Mingming Yang, Ruiqun Chen, Yu Liang, and Weihua Wang; Technical or material support: R.N.V. Krishna Deepak, Yilie Liao, Zhiying Guo, Yunfang Wang, Jiandie D. Lin, and Hao Fan; Data analysis: Lili Cheng, R.N.V. Krishna Deepak, Ziyi Meng, Lei Tao, Junyu Zhang, Yuedong

Huang, Hao Fan, and Ligong Chen; Drafting of the manuscript: Lili Cheng, R.N.V. Krishna Deepak, Hao Fan, and Ligong Chen; R.N.V. Krishna Deepak, Hao Fan, and Ligong Chen obtained the funding for the study; All authors have access to the study data and have reviewed and approved the final manuscript.

ACKNOWLEDGMENTS

The authors thank Lina Xu, Yupei Jiao, Xueying Wang, Yusong Wang, Fang Wei, and Dr. Xiaohui Liu for helping with metabolic flux and lipidomics testing.

FUNDING INFORMATION

This work is supported by the National Natural Science Foundation of China (32130048, 91857108, 92157301, and 31971085 to Ligong Chen), the Ministry of Science and Technology of China National Key R&D Programs (2022YFA0806503, 2018YFA0506903 to Ligong Chen), Tsinghua-Foshan Innovation Special Fund (TFISF, 2020THFS0133 to Ligong Chen), Tsinghua Precision medicine foundation (2022TS013 to Ligong Chen), Tsinghua University Spring Breeze Fund (2021Z99CFY012 to Ligong Chen) and Biomedical Research Council of Agency for Science, Technology, and Research (A*STAR), Singapore to Hao Fan and R.N.V. Krishna Deepak.

CONFLICTS OF INTEREST

The authors have no conflicts of interest to report.

ORCID

Lili Cheng https://orcid.org/0000–0001–8009–1069
R.N.V. Krishna Deepak https://orcid.org/0000–0001–6629–8450
Guoqiang Wang https://orcid.org/0000–0003–4175–3837
Ziyi Meng https://orcid.org/0000–0002–8441–5670
Lei Tao https://orcid.org/0000–0002–6891–5608
Mengqing Xie https://orcid.org/0009–0007–1304–1038
Wenna Chi https://orcid.org/0000–0003–1922–5616
Yuming Zhang https://orcid.org/0009–0002–1406–8906
Mingming Yang https://orcid.org/0009–0007–7972–3349
Yilie Liao https://orcid.org/0009–0008–7122–8690
Ruiqun Chen https://orcid.org/0000–0003–1467–6768
Yu Liang https://orcid.org/0009–0005–3783–6578
Junyu Zhang https://orcid.org/0009–0008–1759–0074
Yuedong Huang https://orcid.org/0000–0001–6262–5880
Weihua Wang https://orcid.org/0000–0002–2996–4490
Zhiying Guo https://orcid.org/0009–0001–2401–8585
Jiandie D. Lin https://orcid.org/0000–0001–8069–5647
Hao Fan https://orcid.org/0000–0003–0199–9752
Ligong Chen https://orcid.org/0000–0002–7893–7173

REFERENCES

1. Ferguson D, Finck BN. Emerging therapeutic approaches for the treatment of NAFLD and type 2 diabetes mellitus. Nat Rev Endocrinol. 2021;17:484–95.
2. Smith BK, Marcinko K, Desjardins EM, Lally JS, Ford RJ, Steinberg GR. Treatment of NAFLD: role of AMPK. Am J Physiol Endocrinol Metab. 2016;311:E730–40.
3. Ford RJ, Fullerton MD, Pinkosky SL, Day EA, Scott JW, Oakhill JS, et al. Metformin and salicylate synergistically activate liver AMPK, inhibit lipogenesis and improve insulin sensitivity. Biochem J. 2015;468:125–32.
4. Fullerton MD, Galic S, Marcinko K, Sikkema S, Pulinilkunnil T, Chen Z-P, et al. Single phosphorylation sites in Acc1 and Acc2 regulate lipid homeostasis and the insulin-sensitizing effects of metformin. Nat Med. 2013;19:1649–54.
5. Wang Y, An H, Liu T, Qin C, Sesaki H, Guo S, et al. Metformin improves mitochondrial respiratory activity through activation of AMPK. Cell Rep. 2019;29:1511–23.
6. Zhang Y, Zhang Y, Sun K, Meng Z, Chen L. The SLC transporter in nutrient and metabolic sensing, regulation, and drug development. J Mol Cell Biol. 2019;11:1–13.
7. Fiermonte G, Leonardis FD, Todisco S, Palmieri L, Lasorsa FM, Palmieri F. Identification of the mitochondrial ATP-Mg/Pi transporter. Bacterial expression, reconstitution, functional characterization, and tissue distribution. J Biol Chem. 2004;279:30722–30.
8. Noia MAD, Todisco S, Cirigliano A, Rinaldi T, Agrimi G, Iacobazzi V, et al. The human SLC25A33 and SLC25A36 genes of solute carrier family 25 encode two mitochondrial pyrimidine nucleotide transporters. J Biol Chem. 2014;289:33137–48.
9. Porcelli V, Fiermonte G, Longo A, Palmieri F. The human gene SLC25A29, of solute carrier family 25, encodes a mitochondrial transporter of basic amino acids. J Biol Chem. 2014;289:13374–84.
10. Tan MGK, Ooi LLPJ, AW SE, Hui KM. Cloning and identification of HCC down-regulated mitochondrial carrier protein, a novel liver-specific uncoupling protein. J Biol Chem. 2004;279:45235–44.
11. Bresciani N, Demagny H, Lemos V, Pontanari F, Li X, Sun Y, et al. The Slc25a47 locus is a novel determinant of hepatic mitochondrial function implicated in liver fibrosis. J Hepatol. 2022;S0168-8278:00364–6.
12. Jin X, Yang Y-d, Chen K, Lv Z-y, Zheng L, Liu Y-p, et al. HDMCP uncouples yeast mitochondrial respiration and alleviates steatosis in L02 and hepG2 cells by decreasing ATP and H2O2 levels: a novel mechanism for NAFLD. J Hepatol. 2009;50:1019–28.
13. Chen L, Shu Y, Liang X, Chen EC, Yee SW, Zur AA, et al. OCT1 is a high-capacity thiamine transporter that regulates hepatic steatosis and is a target of metformin. Proc Natl Acad Sci U S A. 2014;111:9983–8.
14. Cheng L, Ge M, Lan Z, Ma Z, Chi W, Kuang W, et al. Zoledronate dysregulates fatty acid metabolism in renal tubular epithelial cells to induce nephrotoxicity. Arch Toxicol. 2018;92:469–85.
15. Umemura A, Park EJ, Taniguchi K, Lee JH, Shalapour S, Valasek MA, et al. Liver damage, inflammation, and enhanced tumorigenesis after persistent mTORC1 inhibition. Cell Metab. 2014;20:133–44.
16. Xu L, Yang C, Wang J, Li Z, Huang R, Ma H, et al. Persistent mTORC1 activation via Depdc5 deletion results in spontaneous HCC but does not exacerbate carcinogen- and high-fat diet-induced hepatic carcinogenesis in mice. Biochem Biophys Res Commun. 2021;578:142–9.
17. Palmieri F. The mitochondrial transporter family SLC25: identification, properties and physiopathology. Mol Aspects Med. 2013;34:465–84.

18. Pebay-Peyroula E, Dahout-Gonzalez C, Kahn R, Trézéguet V, Lauquin GJ-M, Brandolin G. Structure of mitochondrial ADP/ATP carrier in complex with carboxyatractyloside. Nature. 2003;426:39–44.
19. Jurrus E, Engel D, Star K, Monson K, Brandi J, Felberg LE, et al. Improvements to the APBS biomolecular solvation software suite. Protein Sci. 2018;27:112–28.
20. Nogueiras R, Habegger KM, Chaudhary N, Finan B, Banks AS, Dietrich MO, et al. Sirtuin 1 and sirtuin 3: physiological modulators of metabolism. Physiol Rev. 2012;92:1479–514.
21. Xin T, Lu C. SirT3 activates AMPK-related mitochondrial biogenesis and ameliorates sepsis-induced myocardial injury. Aging. 2020;12:16224–37.
22. Luongo TS, Eller JM, Lu M-J, Niere M, Raith F, Perry C, et al. SLC25A51 is a mammalian mitochondrial NAD^+ transporter. Nature. 2020;588:174–9.
23. Ashkenazy H, Abadi S, Martz E, Chay O, Mayrose I, Pupko T, et al. ConSurf 2016: an improved methodology to estimate and visualize evolutionary conservation in macromolecules. Nucleic Acids Res. 2016;44:W344–50.
24. Rena G, Hardie DG, Pearson ER. The mechanisms of action of metformin. Diabetologia. 2017;60:1577–85.
25. Block RC, Dorsey ER, Beck CA, Brenna JT, Shoulson I. Altered cholesterol and fatty acid metabolism in Huntington disease. J Clin Lipidol. 2010;4:17–23.
26. Seidah NG, Prat A. The multifaceted biology of PCSK9. Endocr Rev. 2022;43:558–82.
27. Inoki K, Kim J, Guan K-L. AMPK and mTOR in cellular energy homeostasis and drug targets. Annu Rev Pharmacol Toxicol 2012;52:381–400.
28. Luo Y-D, Fang L, Yu H-Q, Zhang J, Lin X-T, Liu X-Y, et al. p53 haploinsufficiency and increased mTOR signalling define a subset of aggressive HCC. J Hepatol. 2021;74:96–108.
29. Liu P, Ge M, Hu J, Li X, Che L, Sun K, et al. A functional mammalian target of rapamycin complex 1 signaling is indispensable for c-Myc-driven hepatocarcinogenesis. Hepatology. 2017;66:167–81.
30. Han J, Wang Y. mTORC1 signaling in hepatic lipid metabolism. Protein Cell. 2018;9:145–51.
31. Che L, Chi W, Qiao Y, Zhang J, Song X, Liu Y, et al. Cholesterol biosynthesis supports the growth of hepatocarcinoma lesions depleted of fatty acid synthase in mice and humans. Gut. 2020;69:177–86.
32. Ziegler M, Monné M, Nikiforov A, Agrimi G, Heiland I, Palmieri F. Welcome to the family: identification of the NAD^+ transporter of animal mitochondria as member of the solute carrier family SLC25. Biomolecules. 2021;11:880.
33. Girardi E, Agrimi G, Goldmann U, Fiume G, Lindinger S, Sedlyarov V, et al. Epistasis-driven identification of SLC25A51 as a regulator of human mitochondrial NAD import. Nat Commun. 2020;11:6145.
34. Zhou C-C, Yang X, Hua X, Liu J, Fan M-B, Li G-Q, et al. Hepatic NAD^+ deficiency as a therapeutic target for NAFLD in ageing. Br J Pharmacol. 2016;173:2352–68.
35. Hirschey MD, Shimazu T, Goetzman E, Jing E, Schwer B, Lombard DB, et al. SIRT3 regulates mitochondrial fatty-acid oxidation by reversible enzyme deacetylation. Nature. 2010;464:121–5.
36. Hirschey MD, Shimazu T, Jing E, Grueter CA, Collins AM, Aouizerat B, et al. SIRT3 deficiency and mitochondrial protein hyperacetylation accelerate the development of the metabolic syndrome. Mol Cell. 2011;44:177–90.
37. Zhang T, Liu J, Shen S, Tong Q, Ma X, Lin L. SIRT3 promotes lipophagy and chaperon-mediated autophagy to protect hepatocytes against lipotoxicity. Cell Death Differ. 2020;27:329–44.
38. Li S, Dou X, Ning H, Song Q, Wei W, Zhang X, et al. Sirtuin 3 acts as a negative regulator of autophagy dictating hepatocyte susceptibility to lipotoxicity. Hepatology. 2017;66:936–52.

How to cite this article: Cheng L, Deepak RNVK, Wang G, Meng Z, Tao L, Xie M, et al. Hepatic mitochondrial NAD+ transporter SLC25A47 activates AMPKα mediating lipid metabolism and tumorigenesis. Hepatology. 2023;78:1828–1842. https://doi.org/10.1097/HEP.0000000000000314